

On the Convergence and Calibration of Deep Learning with Differential Privacy

Zhiqi Bu* Hua Wang Qi Long

University of Pennsylvania
 {zbu, wanghua, qlong}@upenn.edu

Abstract

In deep learning with differential privacy (DP), the neural network achieves the privacy usually at the cost of slower convergence (and thus lower performance) than its non-private counterpart. This work gives the first convergence analysis of the DP deep learning, through the lens of training dynamics and the neural tangent kernel (NTK). Our convergence theory successfully characterizes the effects of two key components in the DP training: the per-sample clipping (flat or layerwise) and the noise addition. Our analysis not only initiates a general principled framework to understand the DP deep learning with any network architecture and loss function, but also motivates a new clipping method – the *global clipping*, that significantly improves the convergence, as well as preserves the same DP guarantee and computational efficiency as the existing method, which we term as *local clipping*.

Theoretically speaking, we precisely characterize the effect of per-sample clipping on the NTK matrix and show that the noise level of DP optimizers does not affect the convergence in the *gradient flow* regime, i.e. with infinitesimal learning rate. In particular, we show that the local clipping almost certainly breaks the positive semi-definiteness of NTK, which can be preserved by our global clipping with a properly chosen hyperparameter. Consequently, we show that DP gradient descent (GD) with global clipping converges monotonically to zero loss, which is often violated by the existing DP-GD with local clipping. Notably, our analysis framework easily extends to other optimizers, e.g., DP-Adam. We demonstrate through numerous experiments that DP optimizers equipped with global clipping perform strongly on a wide range of classification and regression tasks. In addition, our global clipping is surprisingly effective at learning *calibrated classifiers*, in contrast to the existing DP classifiers which are oftentimes over-confident and unreliable. Implementation-wise, the new clipping can be realized by inserting one line of code into the Pytorch `Opacus` library.

1 Introduction

Deep learning has achieved tremendous success in many applications that involve crowdsourced information, e.g., face image, emails, financial status, and medical records. However, using such sensitive data raises severe privacy concerns on a range of image recognition, natural language processing and other tasks [10, 49, 44, 18, 19]. For a concrete example, researches have recently demonstrated multiple successful privacy attacks on deep learning models, in which the attackers can re-identify a member in the dataset using the location or the purchase record, via the membership inference attack [50, 12]. In another example, the attackers can extract a person’s name, email address, phone number, and physical address from the billion-parameter GPT-2 [48] via the extraction attack [13]. Therefore, many studies have applied differential privacy (DP) [26, 25, 27, 40, 24, 22], a mathematically rigorous approach, to protect against leakage of private information [1, 39, 38, 30]. To achieve this gold standard of privacy guarantee, since the seminal work [1], DP optimizers are applied to train the neural networks while preserving the accuracy of prediction. To name a few, researchers have proposed DP-SGD [1, 6] and DP-Adam [7] for private deep learning, DP-SGLD [52, 36] for Bayesian neural network, and DP-FedSGD and DP-FedAvg [38] for federated learning.

Algorithmically speaking, DP optimizers generally have two extra steps in comparison to non-DP standard optimizers: the per-sample clipping and the random noise addition, so that DP optimizers descend in the

*Github: https://github.com/woodyx218/opacus_global_clipping.

direction of the averaged, clipped, noisy gradient (see Figure 1). These extra steps protect the resulting models against privacy attacks via the Gaussian mechanism [27, Theorem A.1], at the expense of an empirical performance degradation compared to the non-DP deep learning, in terms of much slower convergence and lower utility. For example, state-of-the-art CIFAR10 accuracy with DP is $\approx 70\%$ without pre-training [45] (while non-DP networks can easily achieve over 90% accuracy) and similar performance drops have been observed on facial images, tweets, and many other datasets [5].

Empirically, many works have evaluated the effects of noise scale, batch size, clipping norm, learning rate, and network architecture on the privacy-accuracy trade-off [1, 45]. However, despite the prevalent usage of DP optimizers, little is known about its convergence behavior from a theoretical viewpoint, which is necessary to understand and improve the deep learning with differential privacy. We notice one previous attempt by [15], analyzing the DP-SGD convergence through an assumption of symmetric gradient distribution, which can be unrealistic and inapplicable to real datasets.

Our Contributions In this work, we establish a principled framework to analyze the dynamics of DP deep learning, which helps demystify the phenomenon of the privacy-accuracy trade-off.

- We explicitly characterize the *general training dynamics* of deep learning with DP gradient methods (e.g., DP-GD and DP-Adam). We show a fundamental influence of the DP training on the NTK matrix, which causes the convergence to worsen. This analysis leads to a *convergence theory* for the DP deep learning.
- On top of our convergence analysis, we propose a novel principle for designing the DP optimizers and thus develop a new *global clipping* method that provably enjoys desirable convergence behaviors.
- We demonstrate via numerous experiments that DP optimizers with global clipping significantly improve the loss convergence. Interestingly, our clipping further effectively mitigates the *calibration* issue of existing DP classifiers, which usually exacerbates the “over-confidence” in non-DP models.
- Global clipping has the *same privacy guarantee, computational efficiency* and *hyperparameter tuning difficulty* as the local clipping. This leads to a *mix-up training* strategy that applies both clippings interchangeably.
- Our global clipping is *easy-to-code* (see Appendix D) and *generalizable* to arbitrary optimizers, network architectures, loss functions, and tasks including the federated learning.

To elaborate on the study of *calibration* [32, 43], a critical performance measure besides accuracy and privacy, we give a concrete example: a binary classifier is calibrated if it predicts with 80% confidence (the probability assigned on its output class) and has an average accuracy close to 80%, i.e., this classifier’s confidence matches its ability. We observe that DP models using the local clipping are oftentimes too over-confident to be reliable, while the global clipping is amazingly effective on mitigating the mis-calibration. A quick preview of the comparison among the DP optimizers with the local and the global clipping is as follows:

Clipping type	Positive NTK	Loss convergence	Monotone loss decay	To zero loss
No clipping	Yes	Yes	Yes	Yes
Local & Flat	No	No	No	Yes
Local & Layerwise	No	No	No	No
Global & Flat	Yes	Yes	Yes	Yes
Global & Layerwise	Yes	Yes	Yes	Yes

Table 1: Effects of different per-sample clippings on deep learning with DP-GD, assuming no screening happens in global clipping. Here “Yes/No” means guaranteed or not and the loss refers to the training set. “Loss convergence” is conditioned on $\mathbf{H}(t) \succ 0$ (see (2.1)).

2 Warmup: Convergence of Non-Private Gradient Descent

We start by reviewing the standard, non-DP Gradient Descent (GD) for *arbitrary neural network* and *arbitrary loss* that can be represented as a sum of per-sample losses, before we dive into the analysis of DP

optimizers. In particular, we analyze the training dynamics of a neural network using the neural tangent kernel (NTK) matrix¹.

Suppose a neural network f is governed by weights \mathbf{w} , with samples \mathbf{x}_i and labels y_i ($i = 1, \dots, n$). Denote the prediction by $f_i = f(\mathbf{x}_i, \mathbf{w})$, and the per-sample loss by $\ell_i = \ell(f(\mathbf{x}_i, \mathbf{w}), y_i)$ for some loss function ℓ . We define the objective function L to be the average of per-sample losses

$$L(\mathbf{w}) = \frac{1}{n} \sum_{i=1}^n \ell(f(\mathbf{x}_i, \mathbf{w}), y_i).$$

The discrete gradient descent, with a step size η , can be written as:

$$\mathbf{w}(k+1) = \mathbf{w}(k) - \eta \frac{\partial L}{\partial \mathbf{w}}^\top.$$

The corresponding *gradient flow*, i.e., the ordinary differential equation (ODE) describing the weight updates with infinitely small step size $\eta \rightarrow 0$ in the continuous time, is then:

$$\dot{\mathbf{w}}(t) = -\frac{\partial L}{\partial \mathbf{w}}^\top = -\frac{1}{n} \sum_i \nabla_{\mathbf{w}} \ell_i(t).$$

Applying the chain rules to the gradient flow, we obtain the following general dynamics of the loss L ,

$$\dot{L} = \frac{\partial L}{\partial \mathbf{w}} \dot{\mathbf{w}} = -\frac{\partial L}{\partial \mathbf{w}} \frac{\partial L}{\partial \mathbf{w}}^\top = -\frac{\partial L}{\partial \mathbf{f}} \frac{\partial \mathbf{f}}{\partial \mathbf{w}} \frac{\partial \mathbf{f}}{\partial \mathbf{w}}^\top \frac{\partial L}{\partial \mathbf{f}} = -\frac{\partial L}{\partial \mathbf{f}} \mathbf{H}(t) \frac{\partial L}{\partial \mathbf{f}}^\top, \quad (2.1)$$

where $\frac{\partial L}{\partial \mathbf{f}} = \frac{1}{n} (\frac{\partial \ell_1}{\partial f_1}, \dots, \frac{\partial \ell_n}{\partial f_n}) \in \mathbb{R}^{1 \times n}$, and the Gram matrix $\mathbf{H}(t) := \frac{\partial \mathbf{f}}{\partial \mathbf{w}} \frac{\partial \mathbf{f}}{\partial \mathbf{w}}^\top \in \mathbb{R}^{n \times n}$ is known as the NTK matrix, which is positive semi-definite and crucial to analyzing the convergence behavior.

To give a concrete example, let ℓ be the MSE loss $\ell_i(\mathbf{w}) = (f(\mathbf{x}_i, \mathbf{w}) - y_i)^2$ and $L_{\text{MSE}} = \frac{1}{n} \sum_i \ell_i(\mathbf{w}) = \frac{1}{n} \sum_i (f_i - y_i)^2$, then $\dot{L}_{\text{MSE}} = -4(\mathbf{f} - \mathbf{y})^\top \mathbf{H}(t)(\mathbf{f} - \mathbf{y})/n^2$. Furthermore, if $\mathbf{H}(t)$ is positive definite, the MSE loss $L_{\text{MSE}} \rightarrow 0$ exponentially fast [23, 2, 54], the cross-entropy loss $L_{\text{CE}} \rightarrow 0$ at rate $O(1/t)$ and any loss convex in the prediction $L = \sum_i \ell_i/n$ converges to 0 [2].

3 Differentially Private Gradient Methods and Global Clipping

We now introduce the DP optimizers [31, 28] to train the DP neural networks. One popular optimizer is the DP-SGD [51, 14, 1, 7] in Algorithm 1 and more optimizers such as DP-Adam and DP-FedAvg [38] for federated learning can be found in Appendix F. In contrast to the standard SGD, the DP-SGD has two unique steps: the per-sample clipping (to bound the sensitivity of per-sample gradients) and the random noise addition (to guarantee the privacy of models), both are discussed in details via the Gaussian mechanism in Lemma 5.2.

Algorithm 1 DP-SGD (with local or global flat per-sample clipping)

Parameters: initial weights \mathbf{w}_0 , learning rate η_t , subsampling probability p , number of iterations T , noise scale σ , gradient norm bound R , maximum norm bound $Z \geq R$.

for $t = 0, \dots, T - 1$ **do**

 Subsample a batch $I_t \subseteq \{1, \dots, n\}$ from training set with probability p

for $i \in I_t$ **do**

$v_t^{(i)} \leftarrow \nabla_{\mathbf{w}} \ell(f(\mathbf{x}_i, \mathbf{w}_t), y_i)$

 Option 1: $C_{\text{local},i} = \min \{1, R/\|v_t^{(i)}\|_2\}$ ▷ Local clipping factor (existing)

 Option 2: $C_{\text{global},i} \equiv \begin{cases} R/Z & \text{if } \|v_t^{(i)}\|_2 \leq Z \\ 0 & \text{if } \|v_t^{(i)}\|_2 > Z \end{cases}$ ▷ Global clipping factor (ours)

$\bar{v}_t^{(i)} \leftarrow C_i \cdot v_t^{(i)}$ ▷ Clip the gradient

$\bar{V}_t \leftarrow \sum_{i \in I_t} \bar{v}_t^{(i)}$ ▷ Sum over batch

$\mathbf{w}_{t+1} \leftarrow \mathbf{w}_t - \frac{\eta_t}{|I_t|} (\bar{V}_t + \sigma R \cdot \mathcal{N}(0, I))$ ▷ Apply Gaussian mechanism and descend

¹We emphasize that our analysis works on any neural networks, not limited to the infinitely wide or over-parameterized ones. Put differently, we don't assume the NTK matrix \mathbf{H} to be deterministic nor nearly time-independent, as was the case in [3, 35, 23, 2, 54, 29, 4].

Although the per-sample clipping is widely applied in DP deep learning, its effect remains a mystery. Empirical observations have found that optimizers with the per-sample clipping (even when no noise is present) have much worse convergence and accuracy [1, 5]. But the current form of clipping is heuristic and lacks theoretical understanding, especially when the noise addition is present. In what follows, we use C to denote C_{local} or C_{global} when it is clear from the context.

We propose and analyze a new clipping, namely the **global clipping** as in Option 2 of Algorithm 1, where the clipping operation takes place on all per-sample gradients that pass the screening procedure. From this viewpoint, the global clipping is a *batch clipping* instead of an individual clipping (see Appendix F.6 for comparison with local clipping). More precisely, in local clipping, each per-sample gradient $\nabla_{\mathbf{w}}\ell_i$ compare its length to R and multiplied with a sample-specific clipping factor $0 < C_i \leq 1$. In global clipping, only $\nabla_{\mathbf{w}}\ell_i$ with norm smaller than Z is used (otherwise $C_i = 0$) and multiplied with a common clipping factor R/Z , which guarantees the sensitivity to be R , same as in local clipping. At the high level, the idea of global clipping is to preserve the gradient direction (i.e. to remove the gradient bias) while bounding the sensitivity during the clipping, which will guarantee the positive semi-definiteness of the NTK matrix via Theorem 2.

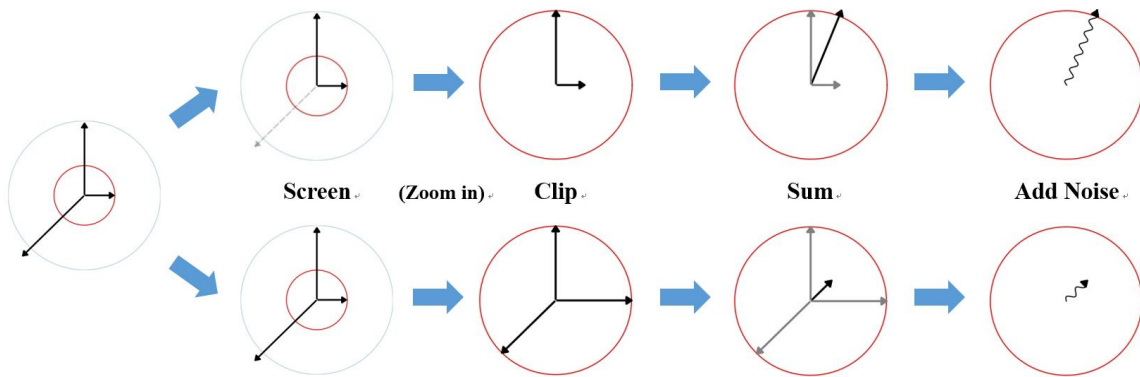


Figure 1: Illustration of global (upper) and local per-sample clipping (lower) in Algorithm 1. The black arrowed lines are three per-sample gradients. The red and grey circles have radius R and Z .

Remark 3.1. We note that our global clipping only requires tuning two hyperparameters (η, Z) , similar to the local clipping where (η, R) require tuning. Therefore, our clipping does not introduce additional tuning difficulty. To see this, we can view the update of our DP-SGD as $\frac{\eta R}{|I_t|} \left(\sum_i \tilde{C}_{global,i} v_t^{(i)} + \sigma \cdot \mathcal{N}(0, I) \right)$ in which $\tilde{C}_{global,i} = 1/Z$ or 0 is independent of R . Consequently, we can always set $R = 1$ in the global clipping.

4 Convergence Analysis of DP Optimizers

In this section, we analyze the weight and loss dynamics of DP optimizers with the local or global per-sample clipping, denoted in the subscript, e.g., DP-SGD_{local} and DP-SGD_{global}. Our narrative here focuses on the most widely used DP-GD for the sake of simplicity, and our analysis generalizes to other full-batch DP optimizers such as DP-HeavyBall, DP-RMSprop, and DP-Adam as well, in Theorem 4 and Appendix F.

4.1 Effect of Noise Addition on Convergence

Our first result is easy yet surprising: the gradient flow of a stochastic noisy GD with non-zero noise (4.1) is the same as that of a deterministic dynamics without the noise (4.2). Put differently, the noise addition has no effect on the convergence of DP optimizers in the continuous time analysis. This is a common phenomenon called *certainty equivalence* in the stochastic control community [16].

To elaborate this point, we consider the DP-GD with Gaussian noise, as in Algorithm 1,

$$\mathbf{w}(k+1) = \mathbf{w}(k) - \frac{\eta}{n} \left(\sum_i \nabla_{\mathbf{w}}\ell_i C_i + \sigma R \cdot \mathcal{N}(0, 1) \right). \quad (4.1)$$

Notice that this general dynamics covers both the non-DP GD ($\sigma = 0$ and $C_i \equiv 1$) and DP-GD with local or global clipping. Through Fact 4.1, we claim that the gradient flow of (4.1) is the same ODE regardless of the value of σ , and prove this in Appendix B.

Fact 4.1. For all $\sigma \geq 0$, the gradient descent in (4.1) corresponds to the continuous gradient flow

$$d\mathbf{w}(t) = -\frac{1}{n} \sum_i \nabla_{\mathbf{w}} \ell_i(t) C_i(t) dt. \quad (4.2)$$

This result indeed aligns the conventional wisdom² of tuning the clipping norm C first (e.g. setting $\sigma = 0.0$ or small) then the noise level σ , since the convergence is more sensitive to the clipping.

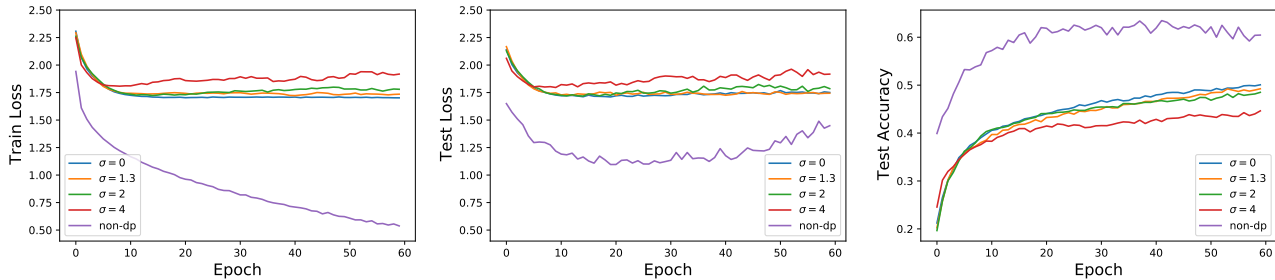


Figure 2: Performance of DP-SGD_{local} with various noise σ on CIFAR10, using same setting as in Section 6.2. Notice that when $\sigma = 0$ and no clipping is applied, test accuracy is about 62%.

Remark 4.2. Our proof of Fact 4.1 shows that the certainty equivalence holds true generally for any DP optimizer besides DP-GD, i.e., different σ results in the same gradient flow as $\eta \rightarrow 0$.

4.2 Effect of Per-Sample Clipping on NTK Matrix

We move on to analyze the effect of the per-sample clipping on the DP training (4.2). It has been empirically observed that the per-sample clipping results in worse convergence and accuracy even without the noise [5]. We highlight that the NTK matrix is the key to understanding the convergence behavior and that the clipping affects NTK through its linear algebra properties, especially the positive semi-definiteness, which we define below in two notions for a *general* matrix.

Definition 4.3. For a (not necessarily symmetric) matrix A , it is

1. *positive in quadratic form* if and only if $\mathbf{x}^\top A \mathbf{x} \geq 0$ for every non-zero \mathbf{x} ;
2. *positive in eigenvalues* if and only if all eigenvalues of A are non-negative.

These two positivity definitions are equivalent for a symmetric or Hermitian matrix, but not so for non-symmetric matrices. We illustrate this difference in Appendix A with some concrete examples. Next, we introduce two styles of per-sample clippings. Both can be implemented locally or globally.

Flat Clipping The DP-GD described in Algorithm 1 and (4.1), with the gradient flow (4.2), is equipped with the *flat* clipping [37]. In words, the flat clipping upper bounds the entire gradient vector by a norm R . Using the chain rules, we get

$$\dot{L} = \frac{\partial L}{\partial \mathbf{w}} \dot{\mathbf{w}} = -\frac{1}{n^2} \sum_j \nabla_{\mathbf{w}} \ell_j \sum_i \nabla_{\mathbf{w}} \ell_i C_i = -\frac{\partial L}{\partial \mathbf{f}} \mathbf{H} \mathbf{C} \frac{\partial L}{\partial \mathbf{f}}^\top, \quad (4.3)$$

where $\mathbf{C}(t) = \text{diag}(C_1, \dots, C_n)$ is the clipping matrix at time t , with C_i defined in Algorithm 1.

²See https://github.com/pytorch/opacus/blob/master/tutorials/building_image_classifier.ipynb

Layerwise Clipping. We additionally analyze another widely used clipping – the *layerwise* clipping [1, 38, 46]. Unlike the flat clipping, the layerwise clipping upper bounds the r -th layer’s gradient vector by a layer-dependent norm R_r , as demonstrated in Algorithm 2. Therefore, the DP-GD and its gradient flow with this layerwise clipping are:

$$\mathbf{w}_r(k+1) = \mathbf{w}_r(k) - \frac{\eta}{n} \left(\sum_i \nabla_{\mathbf{w}_r} \ell_i C_{i,r} + \sigma R_r \cdot \mathcal{N}(0,1) \right) \quad \text{and} \quad \dot{\mathbf{w}}_r(t) = -\frac{1}{n} \sum_i \nabla_{\mathbf{w}_r} \ell_i C_{i,r}.$$

Then the loss dynamics is obtained by the chain rules:

$$\dot{L} = \sum_r \frac{\partial L}{\partial \mathbf{w}_r} \dot{\mathbf{w}}_r = - \sum_r \frac{\partial L}{\partial \mathbf{f}} \mathbf{H}_r \mathbf{C}_r \frac{\partial L}{\partial \mathbf{f}}^\top, \quad (4.4)$$

where the layerwise NTK matrix $\mathbf{H}_r = \frac{\partial \mathbf{f}}{\partial \mathbf{w}_r} \frac{\partial \mathbf{f}}{\partial \mathbf{w}_r}^\top$, and $\mathbf{C}_r(t) = \text{diag}(C_{1,r}, \dots, C_{n,r})$.

In short, from (4.3) and (4.4), the per-sample clipping precisely changes the NTK matrix from $\mathbf{H} \equiv \sum_r \mathbf{H}_r$, in standard non-DP deep learning, to $\mathbf{H}\mathbf{C}$ in DP training with flat clipping, and to $\sum_r \mathbf{H}_r \mathbf{C}_r$ in DP training with layerwise clipping. Subsequently, we will show that this may break the NTK’s positivity and worsen the convergence of DP training than the non-DP one.

4.3 Local Per-Sample Clipping Breaks NTK Positivity

We start with the analysis of local clipping, which is the prevailing clipping technique prior to our work. We show that the DP-GD with local clipping breaks the traditional positive semi-definiteness of the NTK matrix³.

Theorem 1. *For an arbitrary neural network and a loss convex in f , suppose we clip the per-sample gradients **locally** in the gradient flow of DP-GD, and assume $\mathbf{H}(t) \succ 0$, then:*

1. *The local flat clipping has the loss dynamics in (4.3), with NTK matrix $\mathbf{H}(t)\mathbf{C}_{local}(t)$, which may not be symmetric nor positive in quadratic form, but is positive in eigenvalues.*
2. *The local layerwise clipping has the loss dynamics in (4.4), with NTK matrix $\sum_r \mathbf{H}_r(t)\mathbf{C}_{local,r}(t)$, which may not be symmetric nor positive in quadratic form or in eigenvalues.*
3. *For both local flat and layerwise clipping, the loss $L(t)$ may not decrease monotonically.*
4. *If the loss $L(t)$ converges, for the flat clipping, it converges to 0; for the layerwise clipping, it may converge to a non-zero value.*

We prove Theorem 1 in Appendix B. The theorem states that the symmetry of NTK is almost surely broken by the local clipping, and if furthermore the positive definiteness of NTK is broken, then severe issues may arise in the loss convergence, which is depicted in Figure 7 and Figure 9.

4.4 Global Per-Sample Clipping Can Preserve NTK Positivity with Large Z

Now we switch gears to our global clipping. At each iteration when Z is sufficiently large so that no per-sample gradient is screened out, the global clipping clearly corresponds to a symmetric and positive semi-definite NTK matrix $\mathbf{H}(t)\mathbf{C}(t)$ in flat clipping and $\sum_r \mathbf{H}_r(t)\mathbf{C}_r(t)$ in layerwise clipping, since all per-sample gradients share the same clipping factor. As a result, the clipping matrices are indeed scalar in that $\mathbf{C} = C\mathbf{I}$ in (4.3) and $\mathbf{C}_r = C_r\mathbf{I}$ in (4.4). Hence we obtain the following result for the global clipping.

Theorem 2. *For an arbitrary neural network and a loss convex in f , suppose we clip the per-sample gradients **globally** in the gradient flow of DP-GD and that $\|v_t^{(i)}\|_2 \leq Z^4$, assuming $\mathbf{H}(t) \succ 0$, then:*

1. *The global flat (resp. layerwise) clipping has loss dynamics in (4.3) (resp. (4.4)), with NTK matrix $\mathbf{H}(t)\mathbf{C}_{global}(t)$ (resp. $\sum_r \mathbf{H}_r(t)\mathbf{C}_{global,r}(t)$), and both NTK matrices are symmetric and positive definite.*

³It is a fact that the product of a symmetric and positive definite matrices and a positive diagonal matrix may not be symmetric nor positive in quadratic form. This is shown in Appendix A.

⁴If Z is not large and the screening is effective, then the global clipping (flat or layerwise) may break its symmetry and positivity both in quadratic form and in eigenvalues. Consequently, the training loss may not decrease monotonically nor to zero.

2. For both global flat and layerwise clipping, the loss $L(t)$ decreases monotonically to 0.

We prove Theorem 2 in Appendix B and the benefits of the global clipping are assessed in Section 6. Our findings from Theorem 1 and Theorem 2 are visualized in the left plot of Figure 11 and summarized in Table 2, which further leads to Table 1.

Clipping method	NTK matrix	Symmetric matrix	Positive in quadratic form	Positive in eigenvalues
No clipping	$\mathbf{H} \equiv \sum_r \mathbf{H}_r$	Yes	Yes	Yes
Local & Flat	$\mathbf{H}\mathbf{C}$	No	No	Yes
Local & Layerwise	$\sum_r \mathbf{H}_r \mathbf{C}_r$	No	No	No
Global & Flat	$\mathbf{H}\mathbf{C}$	Yes	Yes	Yes
Global & Layerwise	$\sum_r \mathbf{H}_r \mathbf{C}_r$	Yes	Yes	Yes

Table 2: Linear algebra properties of NTK by different clipping methods, assuming no screening happens in global clipping. Here ‘Yes/No’ means guaranteed or not.

4.5 Connection to Bayesian Deep Learning

When Z is sufficiently large and all per-sample gradients are clipped, DP-SGD with global clipping is essentially the SGD with rescaled learning rate and independent Gaussian noise. This is indeed the stochastic gradient langevin dynamics (SGLD) that is widely applied in training Bayesian neural networks. Similarly, DP-HeavyBall with global clipping can be viewed as stochastic gradient Hamiltonian Monte Carlo. This equivalence relation opens new door to understanding DP optimizers by borrowing the rich literature from the Bayesian learning. Especially, the uncertainty quantification of Bayesian neural network implies the amazing calibration given by the global clipping.

5 Privacy Analysis of DP Optimizers

In this section we define DP mathematically and prove that DP optimizers using the global clipping have the **same privacy** guarantee as those using the local clipping. Notice that for the privacy analysis, we work with the general DP optimizers, including those with mini-batches.

Definition 5.1. A randomized algorithm M is (ϵ, δ) -differentially private (DP) if for any neighboring datasets S, S' differ by an arbitrary sample, and for any event E ,

$$\mathbb{P}[M(S) \in E] \leq e^\epsilon \mathbb{P}[M(S') \in E] + \delta. \quad (5.1)$$

A common approach to guarantee DP when approximating a function g is via additive noise calibrated to g 's sensitivity [26]. This is known as the Gaussian mechanism and widely used in DP deep learning.

Lemma 5.2 (Theorem A.1 [27]; Theorem 2.7 [22]). *Define the ℓ_2 **sensitivity** of any function g to be $\Delta g = \sup_{S, S'} \|g(S) - g(S')\|_2$ where the supreme is over all neighboring (S, S') . Then the **Gaussian mechanism** $\hat{g}(S) = g(S) + \sigma \Delta g \cdot \mathcal{N}(0, \mathbf{I})$ is (ϵ, δ) -DP for some ϵ depending on (σ, n, p, δ) .*

For the same differentially private mechanism, different privacy accountants (e.g., Moments accountant [1, 11], Gaussian differential privacy (GDP) [22, 7], Fourier accountant [34], each based on a different composition theory) accumulate the privacy risk $\epsilon(\sigma, n, p, \delta, T)$ differently over T iterations. The next result shows that DP optimizers with global clipping is as private as those with local clipping, independent of the choice of the privacy accountant.

Theorem 3. *DP optimizers with the local or global clipping are equally (ϵ, δ) -DP.*

Proof of Theorem 3. Under local or global clipping in Algorithm 1, each clipped gradient $\bar{v}_t^{(i)}$ has a norm bounded by R . Therefore, both clippings have the same sensitivity of $\bar{V}_t = \sum_{i \in I_t} \bar{v}_t^{(i)}$ and hence the same privacy risk, regardless which privacy accountant is adopted. \square

While a DP model by definition is resilient to all types of privacy attacks, we illustrate that DP-SGD_{global} offers similar privacy protection to DP-SGD_{local} against the membership inference attacks (MIA) in Figure 3. MIA is a common privacy attack by which the attacker aims to determine whether a given data point belongs to the sensitive training set [26, 38, 41, 48]. In our setting, the black-box attacker uses a logistic regression that only has access to the prediction logits and labels. The privacy vulnerability is characterized as the attack model’s AUC, while lower AUC is preferred.

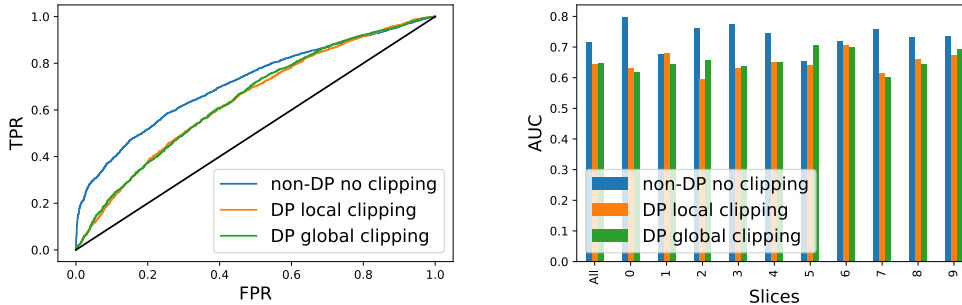


Figure 3: Attack model’s ROC-AUC on entire CIFAR10 in Section 6.2. Upper: non-DP overall AUC, 0.717; DP-SGD_{local}, 0.644; DP-SGD_{global}, 0.648. Lower: AUC on subsets of samples by label classes.

6 Numerical Results

We highlight that the global clipping works with any DP optimizers (e.g., DP-Adam, DP-RMSprop, DP-FTRL[33], DP-SGD-JL[8], etc.) that employ the local clipping, with *almost identical computational complexity* (discussed in Appendix D). Empirically, DP optimizers with global clipping improve over existing DP optimizers on the convergence of training and generalization losses. We thus reveal a novel phenomenon that DP optimizers play important roles in producing well-calibrated and reliable models.

In M -class classification problems, we denote the probability prediction for the i -th sample as $\boldsymbol{\pi}_i \in \mathbb{R}^M$ so that $f(\boldsymbol{x}_i) = \operatorname{argmax}(\boldsymbol{\pi}_i)$, then the accuracy is $\mathbf{1}\{f(\boldsymbol{x}_i) = y_i\}$. The confidence, i.e., the probability associated with the predicted class, is $\hat{P}_i := \max_{k=1}^M [\boldsymbol{\pi}_i]_k$ and a good calibration means the confidence is close to the accuracy⁵. Formally, we employ three popular calibration metrics from [41]: the test loss, i.e. the negative log-likelihood (NLL), the Expected Calibration Error (ECE),

$$\mathbb{E}_{\hat{P}_i} \left[\left| \mathbb{P}(f(\boldsymbol{x}_i) = y_i | \hat{P}_i = p) - p \right| \right],$$

and the Maximum Calibration Error (MCE)

$$\max_{p \in [0,1]} \left| \mathbb{P}(f(\boldsymbol{x}_i) = y_i | \hat{P}_i = p) - p \right|.$$

	ECE %			MCE %		
	non-DP	DP local	DP global	non-DP	DP local	DP global
CIFAR10	13.9	20.0	3.3	20.9	32.0	9.9
SNLI	13.0	22.0	17.6*	34.7	62.5	28.9
MNIST	0.8	2.5	0.5	21.1	50.2	22.8

Table 3: Calibration metrics ECE and MCE by non-DP (no clipping) and DP optimizers. *Note that the SNLI’s DP global stands for mix-up training described in Section 6.3.

Throughout this paper, we use the GDP privacy accountant for the experiments, with Pytorch Opacus library and on a Google Colab P100 GPU. More details are available in Appendix E.

⁵An over-confident classifier, when predicting wrong at one data point, only reduces its accuracy a little but increases its loss significantly due to large $-\log(\pi_{y_i})$, since too little probability is assigned to the true class.

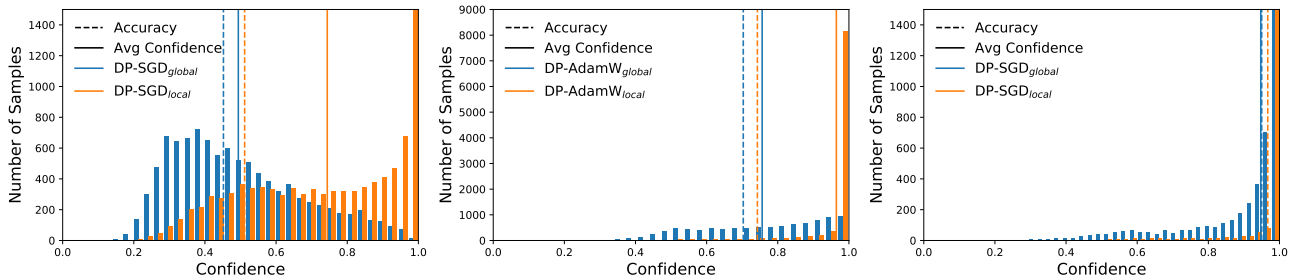


Figure 4: Confidence histograms on CIFAR 10 (left), SNLI (middle), and MNIST (right).

6.1 MNIST image data with CNN model

On the MNIST dataset, which contains 60000 training samples and 10000 test samples of 28×28 grayscale images in 10 classes, we use the standard CNN in the DP libraries⁶[31, 28] (see Appendix E.1 for architecture) and train with DP-SGD. In Figure 5, both clippings result in $(2.32, 10^{-5})$ -DP, similar test accuracy (96% for local and 95% for global), though the global clipping leads to smaller loss (or NLL). In right sub-plot of Figure 5, we demonstrate how Z affects the performance of global clipping, ceteris paribus.

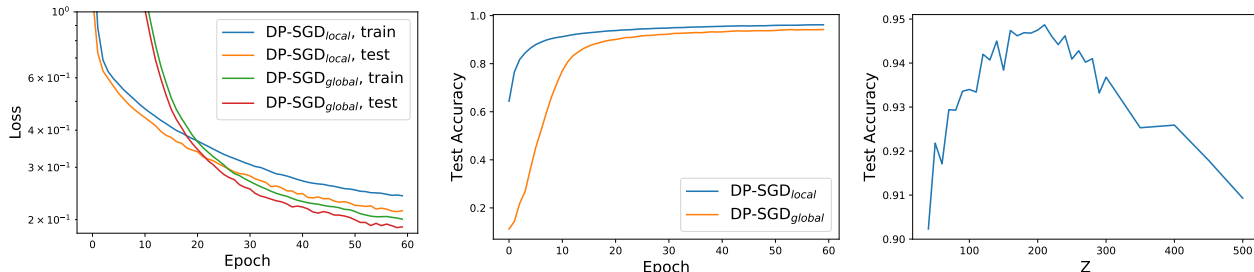


Figure 5: Loss (left) and accuracy (right) on MNIST with 4-layer CNN under different clipping methods, batch size 256, learning rate 0.15, noise scale 1.1, clipping norm 1.0; for global clipping, we choose $Z = 210$ as the maximum gradient bound, $(\epsilon, \delta) = (2.32, 10^{-5})$.

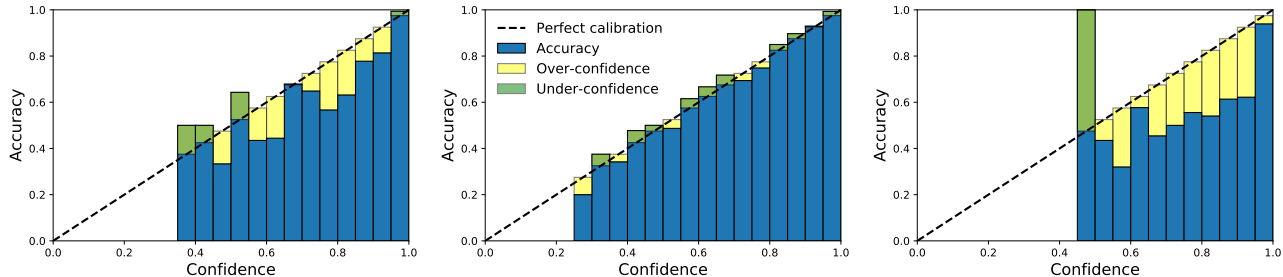


Figure 6: Reliability diagrams (left for non-DP; middle for global clipping; right for local clipping) on MNIST with 4-layer CNN.

In Figure 6, the *reliability diagram* [20, 43] displays the accuracy as a function of confidence. Graphically speaking, a calibrated classifier is expected to have blue bins close to the diagonal black dotted line. While the non-DP model is generally over-confident and thus not calibrated, the global clipping effectively achieves nearly perfect calibration, thanks to its Bayesian learning nature. In contrast, the classifier with local clipping is not only mis-calibrated, but also falls into ‘bipolar disorder’: it is either over-confident and inaccurate, or under-confident but highly accurate. This disorder is observed to different extent in all classification experiments in this paper.

⁶See <https://github.com/tensorflow/privacy/tree/master/tutorials> in Tensorflow and <https://github.com/pytorch/opacus/blob/master/examples/mnist.py> in Pytorch Opacus.

6.2 CIFAR10 image data with CNN model

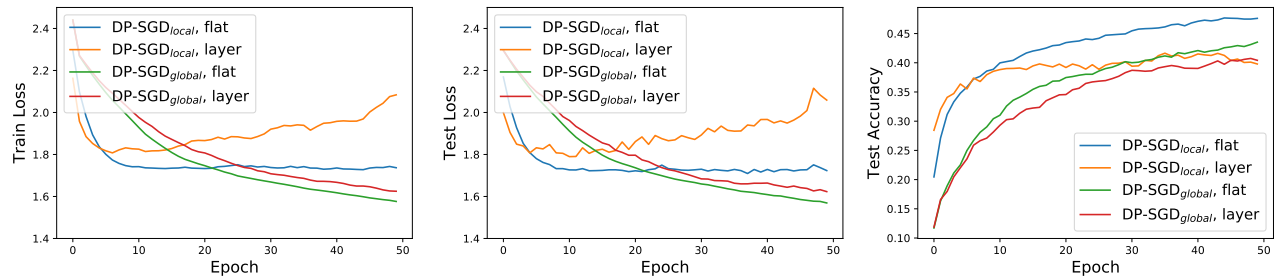


Figure 7: Loss (left and middle) and accuracy (right) on CIFAR10 with 5-layer CNN under different clipping methods, batch size 250, learning rate 0.05, noise scale 1.3, $Z = 75$, clipping norm 1.5 (flat). For layerwise clipping, global: $[1.5, 0.3]$ per layer (1.5 for weights, 0.3 for biases); local: $[1.5, 1.5]$, $(\epsilon, \delta) = (1.96, 10^{-5})$.

CIFAR10 is a more challenging image dataset, which contains 50000 training samples and 10000 test samples of 32×32 color images in 10 classes. We use the standard CNN on Pytorch CIFAR10 tutorial⁷ (see Appendix E.2 for architecture) and train with DP-SGD without pre-training (unlike [1, 53], which pretrain on CIFAR100). Both clippings result in $(1.96, 10^{-5})$ -DP and the test accuracy (local: 47.6%; global: 43.5%; non-DP: 61.3%) is comparable with state-of-the-art in [45], which is around 47% at this privacy budget. Clearly from Figure 7, global clipping has better convergence and similar accuracy than local clipping. Especially, local layerwise clipping can be unstable, as indicated by Theorem 1. Notice that for classification tasks, the inconsistency between the optimization loss (cross-entropy) and the performance measure (accuracy) is not uncommon and even exaggerated in Section 6.3.

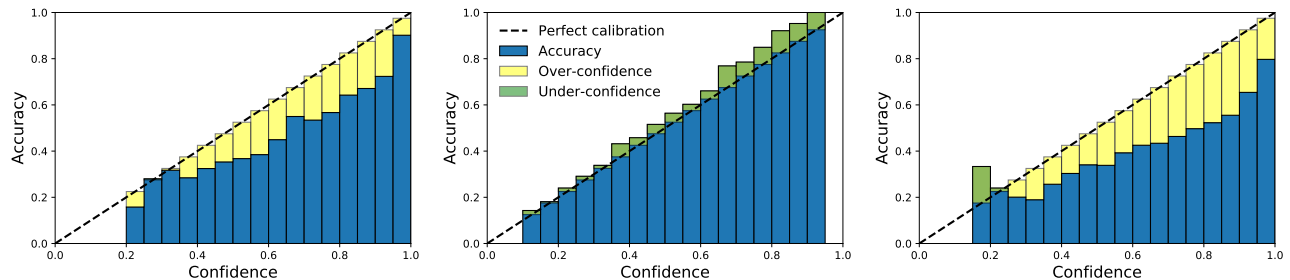


Figure 8: Reliability diagrams (left for non-DP; middle for global clipping; right for local clipping) on CIFAR10 with 5-layer CNN.

As indicated by the higher losses or NLL, the *confidence histogram* in Figure 4 shows the distribution of prediction confidence and validates that DP-SGD_{local} results in poorly calibrated classifiers on CIFAR10 (i.e., its 75.3% confidence is significantly higher than the 47.6% accuracy) but DP-SGD_{global} is well-calibrated.

⁷See https://pytorch.org/tutorials/beginner/blitz/cifar10_tutorial.html.

6.3 SNLI text data with BERT and mix-up training

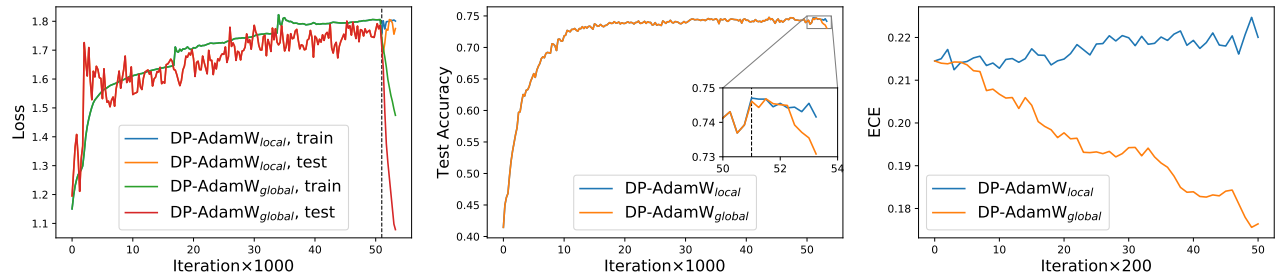


Figure 9: Loss (left), accuracy (middle) and calibration after switching clipping (right) on SNLI with pre-trained BERT, batch size 32, learning rate 0.0005, noise scale 0.4, clipping norm 0.1, $(\epsilon, \delta) = (1.25, 1/550152)$.

Stanford Natural Language Inference (SNLI)⁸ is a collection of human-written English sentence paired with one of three classes: entailment, contradiction, or neutral. The dataset has 550152 training samples and 10000 test samples. We use the pre-trained BERT (Bidirectional Encoder Representations from Transformers) on *Opacus* tutorial⁹, which gives a state-of-the-art privacy-accuracy result. Our BERT contains 108M parameters and we only train the last Transformer encoder, which has 7M parameters, using DP-AdamW. In particular, we use a **mix-up training**: for global clipping, we in fact train BERT with DP-SGD_{local} for 3 epochs (51.5×10^3 iterations) and then use DP-SGD_{global} for an additional 2500 iterations. In other words, 95% of the training is done with local clipping but the last 5% is done with global clipping. For local clipping, DP-SGD_{local} is used for the entire training process of 54076 iterations.

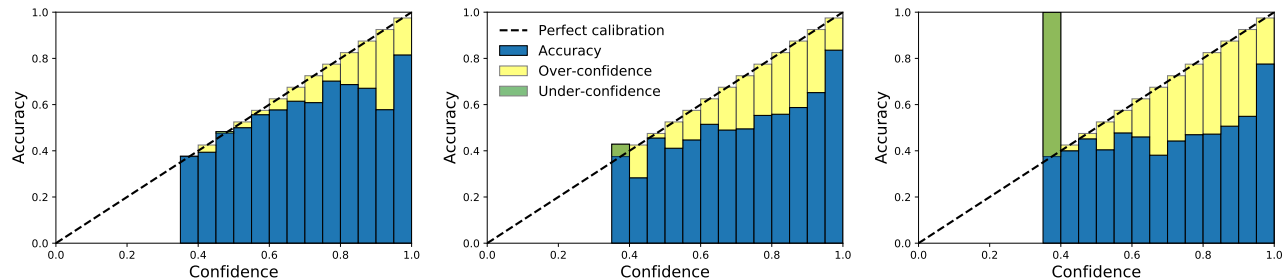


Figure 10: Reliability diagrams (left for non-DP; middle for global clipping; right for local clipping) on SNLI with BERT. Note that global clipping is only used for the last 2500 iterations out of the entire 54000 iterations.

Surprisingly, the existing DP optimizer does not minimize the loss at all, yet the accuracy still improves along the training. We again observe that global clipping has significantly better convergence than the local clipping (observe that when turned to global clipping in the last 2500 steps, the test loss or NLL decreases significantly from 1.79 to 1.08, and the training loss or NLL decreases from 1.81 to 1.47; while keeping local clipping has no effect on reducing the losses). The resulting global model also has similar accuracy (local: 74.1%; global: 73.1%; as a benchmark, non-DP: 85.4%), same privacy ($\epsilon = 1.25, \delta = 1/550152$), and much better calibration in comparison to the local clipping (see Table 3). We remark that all hyperparameters are the same as in the *Opacus* tutorial.

6.4 Regression Tasks

On regression tasks, the performance measure and the loss function are unified as MSE. Figure 11 shows that global clipping is comparable if not better than local clipping. We experiment on the California Housing data (20640 samples, 8 features) and Wine Quality (1599 samples, 11 features, run with full-batch DP-GD). Additional experimental details are available in Appendix E.4.

⁸We use SNLI 1.0 from <https://nlp.stanford.edu/projects/snli/>

⁹See https://github.com/pytorch/opacus/blob/master/tutorials/building_text_classifier.ipynb.

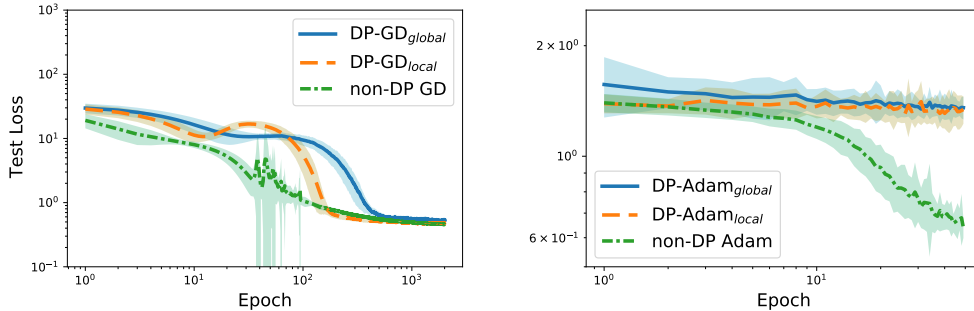


Figure 11: Performance of DP optimizers under different clipping methods on the Wine Quality with $Z = 400$ (left) and the California Housing datasets with $Z = 2000$ (right). Experimental details in Appendix E.4.

7 Discussion

In this paper, we establish a framework of the convergence analysis for DP deep learning, via linear algebra properties of the NTK matrix. Our framework applies to general neural network architecture, loss function, and optimization algorithm. We show that in the continuous time analysis, the noise addition does not affect the convergence but the per-sample clipping does. We then propose the global clipping method, which has provable advantages in convergence with the same privacy guarantee and efficiency as the existing local clipping. Hence, one may apply two clippings interchangeably during the training – a strategy we refer to as mix-up training. Our global clipping significantly outperforms the local clipping in the sense of lower loss and better calibration, while preserving comparable prediction accuracy.

A future direction is to study the discrete time convergence when the learning rate is not small. One immediate observation is that the noise addition will have an effect on the convergence in this case, which needs further investigation. In addition, the more commonly-used mini-batch optimizers require further analysis, where the dynamics is no longer deterministic and instead stochastic differential equation will be analyzed. Another direction is to develop more fine-grained analysis, for instance, on the convergence rate of specific tasks, network architectures, or optimizers. This is an important problem because our current analysis focuses on the terminal phase of training, yet in practice, DP training usually stops before convergence due to the limited privacy budget. Lastly, the inconsistency between the cross-entropy loss and the prediction accuracy, as well as the connection to the calibration issue are intriguing; their theoretical understanding awaits future research.

Acknowledgement

We would like to thank Weijie J. Su, Janardhan Kulkarni, Om Thakkar, and Gautam Kamath for constructive and stimulating discussions, especially around the new global-clipping algorithm. We also thank the **Opacus** team for maintaining this amazing library and for quick response to bugs. This work was supported in part by NIH through R01GM124111 and RF1AG063481.

References

- [1] M. Abadi, A. Chu, I. Goodfellow, H. B. McMahan, I. Mironov, K. Talwar, and L. Zhang. Deep learning with differential privacy. In *Proceedings of the 2016 ACM SIGSAC Conference on Computer and Communications Security*, pages 308–318, 2016.
- [2] Z. Allen-Zhu, Y. Li, and Z. Song. A convergence theory for deep learning via over-parameterization. In *International Conference on Machine Learning*, pages 242–252. PMLR, 2019.
- [3] S. Arora, S. S. Du, W. Hu, Z. Li, R. Salakhutdinov, and R. Wang. On exact computation with an infinitely wide neural net. *arXiv preprint arXiv:1904.11955*, 2019.
- [4] S. Arora, S. S. Du, W. Hu, Z. Li, and R. Wang. Fine-grained analysis of optimization and generalization for overparameterized two-layer neural networks. *arXiv preprint arXiv:1901.08584*, 2019.

- [5] E. Bagdasaryan, O. Poursaeed, and V. Shmatikov. Differential privacy has disparate impact on model accuracy. In *Advances in Neural Information Processing Systems*, pages 15453–15462, 2019.
- [6] R. Bassily, A. Smith, and A. Thakurta. Private empirical risk minimization: Efficient algorithms and tight error bounds. In *2014 IEEE 55th Annual Symposium on Foundations of Computer Science*, pages 464–473. IEEE, 2014.
- [7] Z. Bu, J. Dong, Q. Long, and W. J. Su. Deep learning with gaussian differential privacy. *arXiv preprint arXiv:1911.11607*, 2019.
- [8] Z. Bu, S. Gopi, J. Kulkarni, Y. T. Lee, J. H. Shen, and U. Tantipongpipat. Fast and memory efficient differentially private-sgd via jl projections. *arXiv preprint arXiv:2102.03013*, 2021.
- [9] Z. Bu, S. Xu, and K. Chen. A dynamical view on optimization algorithms of overparameterized neural networks. In *International Conference on Artificial Intelligence and Statistics*, pages 3187–3195. PMLR, 2021.
- [10] C. Cadwalladr and E. Graham-Harrison. Revealed: 50 million facebook profiles harvested for cambridge analytica in major data breach. *The guardian*, 17:22, 2018.
- [11] C. Canonne, G. Kamath, and T. Steinke. The discrete gaussian for differential privacy. *arXiv preprint arXiv:2004.00010*, 2020.
- [12] N. Carlini, C. Liu, Ú. Erlingsson, J. Kos, and D. Song. The secret sharer: Evaluating and testing unintended memorization in neural networks. In *28th {USENIX} Security Symposium ({USENIX} Security 19)*, pages 267–284, 2019.
- [13] N. Carlini, F. Tramer, E. Wallace, M. Jagielski, A. Herbert-Voss, K. Lee, A. Roberts, T. Brown, D. Song, U. Erlingsson, et al. Extracting training data from large language models. *arXiv preprint arXiv:2012.07805*, 2020.
- [14] K. Chaudhuri, C. Monteleoni, and A. D. Sarwate. Differentially private empirical risk minimization. *Journal of Machine Learning Research*, 12(3), 2011.
- [15] X. Chen, S. Z. Wu, and M. Hong. Understanding gradient clipping in private sgd: A geometric perspective. *Advances in Neural Information Processing Systems*, 33, 2020.
- [16] G. C. Chow et al. *Analysis and control of dynamic economic systems*. Wiley, 1975.
- [17] A. B. da Silva and M. Gazeau. A general system of differential equations to model first-order adaptive algorithms. *Journal of Machine Learning Research*, 21(129):1–42, 2020.
- [18] Y.-A. De Montjoye, C. A. Hidalgo, M. Verleysen, and V. D. Blondel. Unique in the crowd: The privacy bounds of human mobility. *Scientific reports*, 3(1):1–5, 2013.
- [19] Y.-A. De Montjoye, L. Radaelli, V. K. Singh, et al. Unique in the shopping mall: On the reidentifiability of credit card metadata. *Science*, 347(6221):536–539, 2015.
- [20] M. H. DeGroot and S. E. Fienberg. The comparison and evaluation of forecasters. *Journal of the Royal Statistical Society: Series D (The Statistician)*, 32(1-2):12–22, 1983.
- [21] N. Ding, Y. Fang, R. Babbush, C. Chen, R. Skeel, and H. Neven. Bayesian sampling using stochastic gradient thermostats. 2014.
- [22] J. Dong, A. Roth, and W. J. Su. Gaussian differential privacy. *arXiv preprint arXiv:1905.02383*, 2019.
- [23] S. S. Du, X. Zhai, B. Póczos, and A. Singh. Gradient descent provably optimizes over-parameterized neural networks. *arXiv preprint arXiv:1810.02054*, 2018.
- [24] J. C. Duchi, M. I. Jordan, and M. J. Wainwright. Local privacy and statistical minimax rates. In *2013 IEEE 54th Annual Symposium on Foundations of Computer Science*, pages 429–438. IEEE, 2013.

- [25] C. Dwork. Differential privacy: A survey of results. In *International conference on theory and applications of models of computation*, pages 1–19. Springer, 2008.
- [26] C. Dwork, F. McSherry, K. Nissim, and A. Smith. Calibrating noise to sensitivity in private data analysis. In *Theory of cryptography conference*, pages 265–284. Springer, 2006.
- [27] C. Dwork, A. Roth, et al. The algorithmic foundations of differential privacy. *Foundations and Trends in Theoretical Computer Science*, 9(3-4):211–407, 2014.
- [28] Facebook. Pytorch Privacy library — Opacus. <https://github.com/pytorch/opacus>.
- [29] S. Fort, G. K. Dziugaite, M. Paul, S. Kharaghani, D. M. Roy, and S. Ganguli. Deep learning versus kernel learning: an empirical study of loss landscape geometry and the time evolution of the neural tangent kernel. *arXiv preprint arXiv:2010.15110*, 2020.
- [30] R. C. Geyer, T. Klein, and M. Nabi. Differentially private federated learning: A client level perspective. *arXiv preprint arXiv:1712.07557*, 2017.
- [31] Google. Tensorflow Privacy library. <https://github.com/tensorflow/privacy>.
- [32] C. Guo, G. Pleiss, Y. Sun, and K. Q. Weinberger. On calibration of modern neural networks. In *International Conference on Machine Learning*, pages 1321–1330. PMLR, 2017.
- [33] P. Kairouz, B. McMahan, S. Song, O. Thakkar, A. Thakurta, and Z. Xu. Practical and private (deep) learning without sampling or shuffling. *arXiv preprint arXiv:2103.00039*, 2021.
- [34] A. Koskela, J. Jälkö, and A. Honkela. Computing tight differential privacy guarantees using fft. In *International Conference on Artificial Intelligence and Statistics*, pages 2560–2569. PMLR, 2020.
- [35] J. Lee, L. Xiao, S. S. Schoenholz, Y. Bahri, R. Novak, J. Sohl-Dickstein, and J. Pennington. Wide neural networks of any depth evolve as linear models under gradient descent. *arXiv preprint arXiv:1902.06720*, 2019.
- [36] B. Li, C. Chen, H. Liu, and L. Carin. On connecting stochastic gradient mcmc and differential privacy. In *The 22nd International Conference on Artificial Intelligence and Statistics*, pages 557–566. PMLR, 2019.
- [37] H. B. McMahan, G. Andrew, U. Erlingsson, S. Chien, I. Mironov, N. Papernot, and P. Kairouz. A general approach to adding differential privacy to iterative training procedures. *arXiv preprint arXiv:1812.06210*, 2018.
- [38] H. B. McMahan, D. Ramage, K. Talwar, and L. Zhang. Learning differentially private recurrent language models. *arXiv preprint arXiv:1710.06963*, 2017.
- [39] F. McSherry and K. Talwar. Mechanism design via differential privacy. In *48th Annual IEEE Symposium on Foundations of Computer Science (FOCS'07)*, pages 94–103. IEEE, 2007.
- [40] I. Mironov. Rényi differential privacy. In *2017 IEEE 30th Computer Security Foundations Symposium (CSF)*, pages 263–275. IEEE, 2017.
- [41] M. P. Naeni, G. Cooper, and M. Hauskrecht. Obtaining well calibrated probabilities using bayesian binning. In *Proceedings of the AAAI Conference on Artificial Intelligence*, volume 29, 2015.
- [42] Y. E. Nesterov. A method for solving the convex programming problem with convergence rate $o(1/k^2)$. In *Dokl. akad. nauk Sssr*, volume 269, pages 543–547, 1983.
- [43] A. Niculescu-Mizil and R. Caruana. Predicting good probabilities with supervised learning. In *Proceedings of the 22nd international conference on Machine learning*, pages 625–632, 2005.
- [44] P. Ohm. Broken promises of privacy: Responding to the surprising failure of anonymization. *UCLA L. Rev.*, 57:1701, 2009.

- [45] N. Papernot, A. Thakurta, S. Song, S. Chien, and Ú. Erlingsson. Tempered sigmoid activations for deep learning with differential privacy. *arXiv preprint arXiv:2007.14191*, 2020.
- [46] N. Phan, X. Wu, H. Hu, and D. Dou. Adaptive laplace mechanism: Differential privacy preservation in deep learning. In *2017 IEEE International Conference on Data Mining (ICDM)*, pages 385–394. IEEE, 2017.
- [47] B. T. Polyak. Some methods of speeding up the convergence of iteration methods. *Ussr computational mathematics and mathematical physics*, 4(5):1–17, 1964.
- [48] A. Radford, J. Wu, R. Child, D. Luan, D. Amodei, and I. Sutskever. Language models are unsupervised multitask learners. *OpenAI blog*, 1(8):9, 2019.
- [49] L. Rocher, J. M. Hendrickx, and Y.-A. De Montjoye. Estimating the success of re-identifications in incomplete datasets using generative models. *Nature communications*, 10(1):1–9, 2019.
- [50] R. Shokri, M. Stronati, C. Song, and V. Shmatikov. Membership inference attacks against machine learning models. In *2017 IEEE Symposium on Security and Privacy (SP)*, pages 3–18. IEEE, 2017.
- [51] S. Song, K. Chaudhuri, and A. D. Sarwate. Stochastic gradient descent with differentially private updates. In *2013 IEEE Global Conference on Signal and Information Processing*, pages 245–248. IEEE, 2013.
- [52] Y.-X. Wang, S. Fienberg, and A. Smola. Privacy for free: Posterior sampling and stochastic gradient monte carlo. In *International Conference on Machine Learning*, pages 2493–2502. PMLR, 2015.
- [53] Z. Xu, S. Shi, A. X. Liu, J. Zhao, and L. Chen. An adaptive and fast convergent approach to differentially private deep learning. In *IEEE INFOCOM 2020-IEEE Conference on Computer Communications*, pages 1867–1876. IEEE, 2020.
- [54] D. Zou, Y. Cao, D. Zhou, and Q. Gu. Gradient descent optimizes over-parameterized deep relu networks. *Machine Learning*, 109(3):467–492, 2020.

A Linear Algebra Facts

Fact A.1. The product $A = M_1 M_2$, where M_1 is a symmetric and positive matrix and M_2 a positive diagonal matrix, is positive definite in eigenvalues but is non-symmetric in general (unless the diagonal matrix is constant) and non-positive in quadratic forms.

Proof of Fact A.1. To see the non-symmetry of A , suppose there exists i, j such that $(M_2)_{jj} \neq (M_2)_{ii}$, then

$$(M_1 M_2)_{ij} = \sum_k (M_1)_{ik} (M_2)_{kj} = (M_1)_{ij} (M_2)_{jj} = (M_1)_{ji} (M_2)_{jj},$$

$$(M_1 M_2)_{ji} = (M_1)_{ji} (M_2)_{ii} \neq (M_1)_{ji} (M_2)_{jj}.$$

Hence A is not symmetric and positive definite. To see that A may be non-positive in the quadratic form, we give a counter-example.

$$M_1 = \begin{pmatrix} 1 & 1 \\ 1 & 2 \end{pmatrix}, M_2 = \begin{pmatrix} 1 & 0 \\ 0 & 0.1 \end{pmatrix}, A = M_1 M_2 = \begin{pmatrix} 1 & 0.1 \\ 1 & 0.2 \end{pmatrix}, (1, -2)A \begin{pmatrix} 1 \\ -2 \end{pmatrix} = -0.4.$$

To see that A is positive in eigenvalues, we claim that an invertible square root $M_1^{1/2}$ exists as M_1 is symmetric and positive definite. Now A is similar to $(M_1^{1/2})^{-1} A M_1^{1/2} = M_1^{1/2} M_2 M_1^{1/2}$, hence the non-symmetric A has the same eigenvalues as the symmetric and positive definite $M_1^{1/2} M_2 M_1^{1/2}$. \square

Fact A.2. Matrix with all eigenvalues positive may be non-positive in quadratic form.

Proof of Fact A.2.

$$A = \begin{pmatrix} -1 & 3 \\ -3 & 8 \end{pmatrix}, (1, 0)A \begin{pmatrix} 1 \\ 0 \end{pmatrix} = -1,$$

though eigenvalues of A are $\frac{1}{2}(7 \pm 3\sqrt{5}) > 0$. \square

Fact A.3. Matrix with positive quadratic forms may have non-positive eigenvalues.

Proof of Fact A.3.

$$A = \begin{pmatrix} 1 & 1 \\ -1 & 1 \end{pmatrix}, (x, y)A \begin{pmatrix} x \\ y \end{pmatrix} = x^2 + y^2 > 0,$$

but eigenvalues of A are $1 \pm i$, not positive nor real. Actually, all eigenvalues of A always have positive real part. \square

Fact A.4. Sum of products of positive definite (symmetric) matrix and positive diagonal matrix may have zero or negative eigenvalues.

Proof of Fact A.4.

$$\mathbf{H}_1 = \begin{pmatrix} 8/9 & 2 \\ 2 & 7 \end{pmatrix}, \quad \mathbf{C}_1 = \begin{pmatrix} 0.9 & 0 \\ 0 & 0.4 \end{pmatrix}, \quad \mathbf{H}_2 = \begin{pmatrix} 3 & 2 \\ 2 & 2 \end{pmatrix}, \quad \mathbf{C}_2 = \begin{pmatrix} 0.1 & 0 \\ 0 & 0.6 \end{pmatrix}.$$

Although \mathbf{H}_j are positive definite, $\mathbf{H}_1 \mathbf{C}_1 + \mathbf{H}_2 \mathbf{C}_2$ has a zero eigenvalue. Further, if $\mathbf{H}_1[1, 1] = 0.7$, $\mathbf{H}_1 \mathbf{C}_1 + \mathbf{H}_2 \mathbf{C}_2$ has a negative eigenvalue. \square

B Details of Main Results

B.1 Proofs of main results

Proof of Fact 4.1. Expanding the discrete dynamic in (4.1) as $\mathbf{w}(k+1) = \mathbf{w}(k) - \frac{\eta}{n} \sum_i \nabla_{\mathbf{w}} \ell_i C_i - \frac{\eta \sigma R}{n} \mathcal{N}(0, 1)$, and chaining it for $r \geq 1$ times, we obtain

$$\mathbf{w}(k+r) - \mathbf{w}(k) = - \sum_{j=0}^{r-1} \frac{\eta}{n} \sum_i \nabla_{\mathbf{w}} \ell_i(\mathbf{w}(k+j)) C_i - \sum_{j=0}^{r-1} \frac{\eta \sigma R}{n} \mathcal{N}(0, 1).$$

In the limit of $\eta \rightarrow 0$, we re-index the weights \mathbf{w} by time, with $t = k\eta$ and $s = r\eta$. Then the left hand side becomes $\mathbf{w}(t+s) - \mathbf{w}(t)$; the first summation on the right hand side converges to $-\frac{1}{n} \int_t^{t+s} \sum_i \nabla_{\mathbf{w}} \ell_i(\tau) C_i(\tau) d\tau$, as long as the integral exists, and the second summation $J(\eta) = \sum_{j=0}^{r-1} \frac{\eta \sigma R}{n} \mathcal{N}(0, 1)$ has

$$\mathbb{E}[J(\eta)] = 0 \quad \text{and} \quad \text{Var}(J(\eta)) = \frac{\sigma^2 R^2 \eta^2}{n^2} r = \eta s \frac{\sigma^2 R^2}{n^2} \rightarrow 0, \text{ as } \eta \rightarrow 0.$$

Therefore, as $\eta \rightarrow 0$, the discrete stochastic dynamic (4.1) converges to a deterministic gradient flow given by the integral

$$\mathbf{w}(t) - \mathbf{w}(0) = -\frac{1}{n} \int_0^t \sum_i \nabla_{\mathbf{w}} \ell_i(\tau) C_i(\tau) d\tau,$$

which corresponds to the ordinary differential equations (4.2). \square

Proof of Theorem 1. We prove the statements using the derived gradient flow dynamics (4.2).

For Statement 1, from our narrative in Section 4.2 and Table 2, we know that the local flat clipping algorithm has $\mathbf{H}(t)\mathbf{C}(t)$ as its NTK. Since $\mathbf{H}(t)$ is positive definite and $\mathbf{C}(t)$ is a positive diagonal matrix, by Fact A.1, the product $\mathbf{H}(t)\mathbf{C}(t)$ is positive in eigenvalues, yet may be asymmetric and not positive in quadratic form in general.

Similarly, for Statement 2, we know the NTK of local layerwise clipping has the form $\sum_r \mathbf{H}_r(t)\mathbf{C}_r(t)$, which by Fact A.4 is asymmetric in general, and may be not positive in quadratic form nor positive in eigenvalues.

For Statement 3, by the training dynamics (4.3) for the local flat clipping algorithm and (4.4) for the local layerwise clipping, we see that \dot{L} equal the negation of a quadratic form of the corresponding NTK. By statement 1 & 2 of this theorem, such quadratic form may not be positive at all t , and hence the loss $L(t)$ is not guaranteed to decrease monotonically.

Lastly, for Statement 4, suppose $L(t)$ converges, i.e. $\dot{L} = 0 = \frac{\partial L}{\partial \mathbf{f}} \dot{\mathbf{f}}$. Suppose we have $L > 0$, then $\frac{\partial L}{\partial \mathbf{f}} \neq 0$ since L is convex in the prediction \mathbf{f} . In this case, we know $\dot{\mathbf{f}} = 0$. Observe that

$$0 = \dot{\mathbf{f}} = \frac{\partial \mathbf{f}}{\partial \mathbf{w}} \frac{\partial \mathbf{w}}{\partial t} = -\frac{\partial \mathbf{f}}{\partial \mathbf{w}} \frac{\partial \mathbf{f}}{\partial \mathbf{w}}^\top \frac{\partial L}{\partial \mathbf{f}}^\top.$$

For the local flat clipping, the NTK matrix, $\frac{\partial \mathbf{f}}{\partial \mathbf{w}} \frac{\partial \mathbf{f}}{\partial \mathbf{w}}^\top = \mathbf{H}\mathbf{C}$ is positive in eigenvalues (by Statement 1), so it could only be the case that $\frac{\partial L}{\partial \mathbf{f}} = \mathbf{0}$, contradicting to our premise that $L > 0$. Therefore we know $L = 0$ as long as it converges for the local flat clipping. On the other hand, for the local layerwise clipping, the NTK may be not positive in eigenvalues. Hence it is possible that $L \neq 0$ when $\dot{L} = 0$. \square

Proof of Theorem 2. The proof is similar to the previous proof, we consider the gradient flow dynamic for global clipping as follows:

For the first statement, we note that the NTKs for global clipping are obviously symmetric: since C and C_r are scalars, we have $(\mathbf{H}(t)C(t))^\top = \mathbf{H}(t)C(t)$, and $(\sum_r \mathbf{H}_r(t)C_r(t))^\top = \sum_r \mathbf{H}_r(t)C_r(t)$, are all symmetric matrices. Also, for all $x \neq 0$, $x^\top \mathbf{H}C x = C \cdot x^\top \mathbf{H}x > 0$, so the symmetric matrix $\mathbf{H}C$ is positive definite. Similar argument can easily show that the summation of symmetric positive matrices is also a positive definite matrix.

Now, to prove the second statement, we note that for both global flat clipping and global layerwise clipping, (4.3) and (4.4) give $\dot{L}(t) < 0$ since the NTKs are positive in quadratic form. That means L decreases monotonically. Additionally, L is bounded below by zero. Therefore L must converge and thus $\dot{L} = 0$. Note that when we have $\frac{\partial L}{\partial \mathbf{f}} = \mathbf{0}$, it implies all $\ell_i = 0$, and thus $L = 0$. \square

C Layerwise Per-Sample Clipping

We elaborate the details of layerwise clipping in this section. We describe the layerwise clipping algorithm for DP-SGD, in complement to Algorithm 1 (not an generalization, i.e. flat clipping is not a subset of layerwise clipping). For other optimizers the extension to layerwise clipping is similar. Assume the neural network has d layers, denote the weights of the r -th layer as \mathbf{w}_r , then the layerwise clipping can clip the per-sample gradient of each layer either locally or globally.

Algorithm 2 DP-SGD (with local or global layerwise per-sample clipping)

Input: Dataset $S = \{(\mathbf{x}_1, y_1), \dots, (\mathbf{x}_n, y_n)\}$, loss function $\ell(f(\mathbf{x}_i, \mathbf{w}_t), y_i)$.

Parameters: initial weights \mathbf{w}_0 , learning rate η_t , subsampling probability p , number of iterations T , noise scale σ , gradient norm bound R_r , maximum norm bound Z_r for each layer $1 \leq r \leq d$.

for $t = 0, \dots, T - 1$ **do**

 Take a subsample $I_t \subseteq \{1, \dots, n\}$ from training set D with subsampling probability p

for $r = 1, \dots, d$ **do**

for $i \in I_t$ **do**

$v_{r,t}^{(i)} \leftarrow \nabla_{\mathbf{w}_r} \ell(f(\mathbf{x}_i, \mathbf{w}_t), y_i)$

 Option 1: $C_{local,(i,r)} = \min \{1, R_r / \|v_{r,t}^{(i)}\|_2\}$ ▷ Local clipping factor

 Option 2: $C_{global,(i,r)} \equiv \begin{cases} R_r / Z_r & \text{if } \|v_{r,t}^{(i)}\|_2 \leq Z_r \\ 0 & \text{if } \|v_{r,t}^{(i)}\|_2 > Z_r \end{cases}$ ▷ Global clipping factor

$\bar{v}_{r,t}^{(i)} \leftarrow C_{i,r} \cdot v_{r,t}^{(i)}$ ▷ Clip the gradient

$\bar{V}_{r,t} \leftarrow \sum_{i \in I_t} \bar{v}_{r,t}^{(i)}$ ▷ Sum over batch

$\tilde{V}_{r,t} \leftarrow \bar{V}_{r,t} + \sigma R_r \cdot \mathcal{N}(0, I)$ ▷ Apply Gaussian mechanism

$\mathbf{w}_{r,t+1} \leftarrow \mathbf{w}_{r,t} - \frac{\eta_t}{|I_t|} \tilde{V}_{r,t}$ ▷ Descend

Output $\mathbf{w}_{r,T}$

For implementation, one can set `max_grad_norm` as a list of scalars in the `Opacus PrivacyEngine`¹⁰.

D Code Implementation

Building on top of the Pytorch `Opacus`¹¹ library, we only need to add one line of code into

https://github.com/pytorch/opacus/blob/master/opacus/per_sample_gradient_clip.py

To understand our implementation, we can equivalently view Option 2 in Algorithm 1 as

$$C_{global,i} = \begin{cases} R/Z & \text{if } C_{local,i} \geq R/Z \\ 0 & \text{if } C_{local,i} < R/Z \end{cases}$$

In this formulation, we can easily implement our global clipping by leveraging the `Opacus` library (which already computes $C_{local,i}$). This can be realized in multiple ways.

For example, we can add the following one line after line 179 (within the for loop),

```
import config;clip_factor=torch.where(clip_factor > self.norm_clipper.thresholds[0]/config.Z,
torch.ones_like(clip_factor)*self.norm_clipper.thresholds[0]/config.Z,
torch.zeros_like(clip_factor))
```

Here we use the package `config` to pass global variable, the maximum norm bound Z . An equivalent but easier-to-follow version is

¹⁰See https://github.com/pytorch/opacus/blob/e9983eced87619f683d84861c6503aca4e9287d1/opacus/privacy_engine.py

¹¹see <https://github.com/pytorch/opacus> as for 2021/09/09.

```

import config;
R=self.norm_clipper.thresholds[0]
Z=config.Z
clip_factor=torch.where(clip_factor > R/Z,
torch.ones_like(clip_factor)*R/Z,
torch.zeros_like(clip_factor))

```

Comparing to the original PyTorch implementation, our code only computes an additional thresholding over B (batch size) values, the extra computational complexity is negligible.

E Experimental Details

E.1 MNIST

For MNIST, we use the standard CNN in `Tensorflow Privacy` and `Opacus`, as listed below. For both global and local clippings, the training hyperparameters (e.g. batch size) in Section 6.1 are exactly the same as reported in <https://github.com/tensorflow/privacy/tree/master/tutorials>, which gives 96.6% accuracy for the local clipping in Tensorflow and similar accuracy in Pytorch, where our experiments are conducted. The non-DP network is about 99% accurate. Notice the tutorial uses a different privacy accountant than the GDP that we used.

```

class SampleConvNet(nn.Module):
    def __init__(self):
        super().__init__()
        self.conv1 = nn.Conv2d(1, 16, 8, 2, padding=3)
        self.conv2 = nn.Conv2d(16, 32, 4, 2)
        self.fc1 = nn.Linear(32 * 4 * 4, 32)
        self.fc2 = nn.Linear(32, 10)

    def forward(self, x):
        # x of shape [B, 1, 28, 28]
        x = F.relu(self.conv1(x)) # -> [B, 16, 14, 14]
        x = F.max_pool2d(x, 2, 1) # -> [B, 16, 13, 13]
        x = F.relu(self.conv2(x)) # -> [B, 32, 5, 5]
        x = F.max_pool2d(x, 2, 1) # -> [B, 32, 4, 4]
        x = x.view(-1, 32 * 4 * 4) # -> [B, 512]
        x = F.relu(self.fc1(x)) # -> [B, 32]
        x = self.fc2(x) # -> [B, 10]
        return x

```

E.2 CIFAR10 with 5-layer CNN

In Section 6.2, we adopt the model from Pytorch tutorial in https://pytorch.org/tutorials/beginner/blitz/cifar10_tutorial.html, which is the following 5-layer CNN.

```

class Net(nn.Module):
    def __init__(self):
        super().__init__()
        self.conv1 = nn.Conv2d(3, 6, 5)
        self.pool = nn.MaxPool2d(2, 2)
        self.conv2 = nn.Conv2d(6, 16, 5)
        self.fc1 = nn.Linear(16 * 5 * 5, 120)
        self.fc2 = nn.Linear(120, 84)
        self.fc3 = nn.Linear(84, 10)

    def forward(self, x):

```

```

x = self.pool(F.relu(self.conv1(x)))
x = self.pool(F.relu(self.conv2(x)))
x = torch.flatten(x, 1) # flatten all dimensions except batch
x = F.relu(self.fc1(x))
x = F.relu(self.fc2(x))
x = self.fc3(x)
return x

```

In addition to Figure 4 and Figure 8, we plot in Figure 12 the distribution of prediction probability on the true class, say $[\pi_i]_{y_i}$ for the i -th sample (notice that Figure 4 plots $\max_k[\pi_i]_k$). Clearly the local clipping gives overly confident prediction: almost half of the time the true class is assigned close to zero prediction probability. The global clipping has a much more balanced prediction probability.

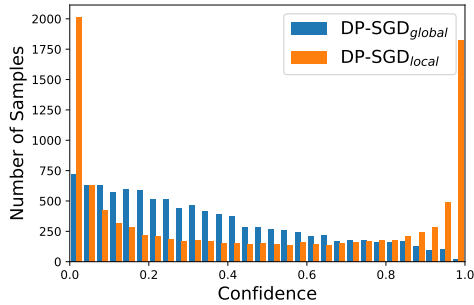


Figure 12: Prediction probability on the true class on CIFAR10 with 5-layer CNN.

E.3 NLP: SNLI with BERT model

In Section 6.3, we use the model from Opacus tutorial in https://github.com/pytorch/opacus/blob/master/tutorials/building_text_classifier.ipynb. The BERT architecture can be found in <https://github.com/pytorch/opacus/blob/master/tutorials/img/BERT.png>.

To train the BERT model, we do the standard pre-processing on the corpus (tokenize the input, cut or pad each sequence to `MAX_LENGTH = 128`, and convert tokens into unique IDs). We train the BERT model for 3 epochs. Similar to Appendix E.2, in addition to Figure 9 and Figure 10, we plot the distribution of prediction probability on the true class in Figure 13. Again, the local clipping is overly confident, with probability masses concentrating on the two extremes, yet the global clipping is more balanced in assigning the prediction probability.

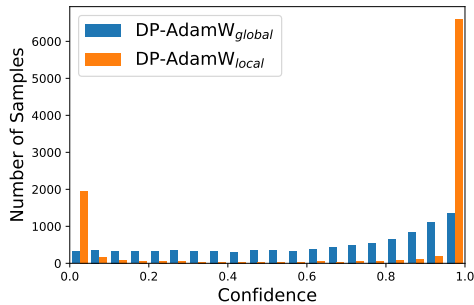


Figure 13: Prediction probability on the true class on SNLI with BERT.

E.4 Regression Experiments

We experiment on the Wine Quality¹² (1279 training samples, 320 test samples, 11 features) and California Housing¹³ (18576 training samples, 2064 test samples, 8 features) datasets in Section 6. For the California Housing, we use DP-Adam with batch size 256. Since other datasets are not large, we use the full-batch DP-GD.

Across all the two experiments, we set $\delta = \frac{1}{1.1 \times \text{training sample size}}$ and use the four-layer neural network with the following structure, where `input_width` is the input dimension for each dataset:

```
class Net(nn.Module):
    def __init__(self, input_width):
        super(StandardNet, self).__init__()
        self.fc1 = nn.Linear(input_width, 64, bias = True)
        self.fc2 = nn.Linear(64, 64, bias = True)
        self.fc3 = nn.Linear(64, 32, bias = True)
        self.fc4 = nn.Linear(32, 1, bias = True)

    def forward(self, x):
        x = F.relu(self.fc1(x))
        x = F.relu(self.fc2(x))
        x = F.relu(self.fc3(x))
        return self.fc4(x)
```

The California Housing dataset is used to predict the mean price value of owner-occupied home in California. We train both global flat and local flat clipping with DP-Adam, both with noise $\sigma = 1$, clipping norm 1, and learning rate 0.0002. We also trained a non-DP GD with the same learning rate. The GDP accountant gives $\epsilon = 4.41$ after 50 epochs / 3650 iterations.

The UCI Wine Quality (red wine) dataset is used to predict the wine quality (an integer score between 0 and 10). We train both global flat and local flat clipping with DP-GD, both with noise $\sigma = 35$, clipping norm 2, and learning rate 0.03. We also trained a non-DP GD with learning rate 0.001. The GDP accountant gives $\epsilon = 4.40$ after 2000 iterations.

The California Housing and Wine Quality experiments are conducted in 30 independent runs. In Figure 11, the lines are the average losses and the shaded regions are the standard deviations.

F Optimizers with Clipping beyond Gradient Descent

We can extend Theorem 1 and Theorem 2 to a wide class of full-batch optimizers besides DP-GD (with $\sigma = 0$ and $\sigma \neq 0$). We show that the NTK matrices in these optimizers determine whether the loss is zero if the model converges.

Theorem 4. *For an arbitrary neural network and a loss convex in f , suppose we clip the per-sample gradients in the gradient flow of Heavy Ball (HB), Nesterov Accelerated Gradient (NAG), Adam, AdaGrad, RMSprop or their DP variants and that $\|v_t^{(i)}\|_2 \leq Z$, assuming $\mathbf{H}(t) \succ 0$, then*

1. *if the loss $L(t)$ converges, it must converge to 0 for local flat, global flat and global layerwise clipping;*
2. *even if the loss $L(t)$ converges, it may converge to non-zero for local layerwise clipping.*

The proof can be easily extracted from that of Theorem 1 and Theorem 2 and hence is omitted. We highlight that DP optimizers in general correspond to deterministic gradient flow (for DP-GD, see Fact 4.1) – as long as the noise injected in each step is linear in step size. Therefore, the gradient flow is the same whether $\sigma > 0$ (the noisy case) or $\sigma = 0$ (the noiseless case).

We also note that the only difference between layerwise clipping and flat clipping is the form of NTK kernel, as we showed in Theorem 1 and Theorem 2. In this section, we will only present the result for flat clipping since its generalization to layerwise clipping is straightforward. In fact, part of the results for the global clipping

¹²<http://archive.672ics.uci.edu/ml/datasets/Wine+Quality>

¹³<http://lib.stat.cmu.edu/datasets/houses.zip>

has been implied by [9], which establishes the error dynamics for HB and NAG, but only on MSE loss and on specific network architecture. To analyze a broader class of optimizers and on the general loss and architecture, we turn to [17] which gives the dynamical systems of all optimizers aforementioned.

F.1 Gradient Methods with Momentum

We study two commonly used momentums, the Heavy Ball [47] and the Nesterov’s one [42]. These gradient methods correspond to the gradient flow system [17, Equation (2.1)]

$$\dot{\mathbf{w}}(t) = -\mathbf{m}(t), \tag{F.1}$$

$$\dot{\mathbf{m}}(t) = \sum_i \nabla_{\mathbf{w}} \ell_i C_i - r(t)\mathbf{m}(t). \tag{F.2}$$

We note that HB corresponds to time-independent $r(t) = r$ for some r and NAG corresponds to $r(t) = 3/t$. At the stationary point, we have $\dot{L} = \dot{\mathbf{w}} = \dot{\mathbf{m}} = 0$. Consequently (F.1) gives $\mathbf{m} = \mathbf{0}$ and (F.2) gives

$$\sum_i \nabla_{\mathbf{w}} \ell_i C_i = r\mathbf{m} = \mathbf{0}. \tag{F.3}$$

Multiplying both sides with $\frac{\partial \mathbf{f}}{\partial \mathbf{w}}$, we get

$$\mathbf{HC} \frac{\partial L}{\partial \mathbf{f}} = \mathbf{0},$$

where $\frac{\partial L}{\partial \mathbf{f}}$ is defined in (4.3). If the NTK is positive in eigenvalues, as is the case for local flat and global clipping, we get $\frac{\partial L}{\partial \mathbf{f}} = \mathbf{0}$ and $\ell_i = 0$ for all i since the loss is convex (thus the only stationary point is the global minimum 0). Hence $L = 0$. Otherwise, e.g. for local layerwise clipping, it is possible that $\frac{\partial L}{\partial \mathbf{f}}^\top \neq \mathbf{0}$ and $L \neq 0$.

F.2 Adaptive Gradient Methods with Momentum

We consider Adam which corresponds to the dynamical system in [17, Equation (2.1)]

$$\dot{\mathbf{w}}(t) = -\mathbf{m}(t)/\sqrt{\mathbf{v}(t) + \xi}, \tag{F.4}$$

$$\dot{\mathbf{m}}(t) = \sum_i \nabla_{\mathbf{w}} \ell_i C_i - \frac{1}{\alpha_1} \mathbf{m}(t), \tag{F.5}$$

$$\dot{\mathbf{v}}(t) = \frac{1}{\alpha_2} \left[\sum_i \nabla_{\mathbf{w}} \ell_i C_i \right]^2 - \frac{1}{\alpha_2} \mathbf{v}(t). \tag{F.6}$$

Here $\xi \geq 0$ and the square is taken elementwise. At the stationary point, we have $\dot{L} = \dot{\mathbf{w}} = \dot{\mathbf{m}} = \dot{\mathbf{v}} = 0$. Consequently (F.4) gives $\mathbf{m} = \mathbf{0}$ and (F.5) gives $\sum_i \nabla_{\mathbf{w}} \ell_i C_i = \mathbf{m}/\alpha_1 = \mathbf{0}$. Multiplying both sides with $\frac{\partial \mathbf{f}}{\partial \mathbf{w}}$, we get again $\mathbf{HC} \frac{\partial L}{\partial \mathbf{f}} = \mathbf{0}$, and hence the results follow.

F.3 Adaptive Gradient Methods without Momentum

We consider ADAGRAD and RMSprop which correspond to the dynamical system in [17, Remark 1]

$$\dot{\mathbf{w}}(t) = -\sum_i \nabla_{\mathbf{w}} \ell_i C_i / \sqrt{\mathbf{v}(t) + \xi}, \tag{F.7}$$

$$\dot{\mathbf{v}}(t) = p(t) \left[\sum_i \nabla_{\mathbf{w}} \ell_i C_i \right]^2 - q(t)\mathbf{v}(t), \tag{F.8}$$

for some $p(t), q(t)$. At the stationary point, we have $\dot{L} = \dot{\mathbf{w}} = \dot{\mathbf{m}} = \dot{\mathbf{v}} = 0$. Consequently (F.7) gives $\sum_i \nabla_{\mathbf{w}} \ell_i C_i = \mathbf{0}$. Multiplying both sides with $\frac{\partial \mathbf{f}}{\partial \mathbf{w}}$, we get again $\mathbf{HC} \frac{\partial L}{\partial \mathbf{f}} = \mathbf{0}$, and hence the results follow.

F.4 Applying Global Clipping to DP Optimization Algorithms

Here we give some concrete algorithms where we can apply the global clipping method.

Many DP optimizers, non-adaptive (like HeavyBall and Nesterov Accelerated Gradient) and adaptive (like Adam, ADAGRAD), can use the global clipping easily. These optimizers are supported in `Opacus` and `Tensorflow Privacy` libraries. The original form of DP-Adam can be found in [7].

Algorithm 3 DP-Adam (with local or global per-sample clipping)

Input: Dataset $S = \{(\mathbf{x}_1, y_1), \dots, (\mathbf{x}_n, y_n)\}$, loss function $\ell(f(\mathbf{x}_i, \mathbf{w}_t), y_i)$.

Parameters: initial weights \mathbf{w}_0 , learning rate η_t , subsampling probability p , number of iterations T , noise scale σ , gradient norm bound R , maximum norm bound Z , momentum parameters (β_1, β_2) , initial momentum m_0 , initial past squared gradient u_0 , and a small constant $\xi > 0$.

for $t = 0, \dots, T - 1$ **do**

 Take a subsample $I_t \subseteq \{1, \dots, n\}$ from training set D with subsampling probability p

for $i \in I_t$ **do**

$v_t^{(i)} \leftarrow \nabla_{\mathbf{w}} \ell(f(\mathbf{x}_i, \mathbf{w}_t), y_i)$

 Option 1: $C_{local,i} = \min \{1, R/\|v_t^{(i)}\|_2\}$ ▷ Local clipping factor

 Option 2: $C_{global,i} \equiv \begin{cases} R/Z & \text{if } \|v_t^{(i)}\|_2 \leq Z \\ 0 & \text{if } \|v_t^{(i)}\|_2 > Z \end{cases}$ ▷ Global clipping factor

$\bar{v}_t^{(i)} \leftarrow C_i \cdot v_t^{(i)}$ ▷ Clip the gradient

$\tilde{V}_t \leftarrow \frac{1}{|I_t|} \left(\sum_{i \in I_t} \bar{v}_t^{(i)} + \sigma R \cdot \mathcal{N}(0, I) \right)$ ▷ Apply Gaussian mechanism

$m_t \leftarrow \beta_1 m_{t-1} + (1 - \beta_1) \tilde{V}_t$

$u_t \leftarrow \beta_2 u_{t-1} + (1 - \beta_2) (\tilde{V}_t \odot \tilde{V}_t)$ ▷ \odot is the Hadamard product

$\mathbf{w}_{t+1} \leftarrow \mathbf{w}_t - \eta_t m_t / (\sqrt{u_t} + \xi)$ ▷ Descend

Output \mathbf{w}_T

Recently, [8] proposes to accelerate many DP optimizers with the JL projections in a memory efficient manner. Examples include DP-SGD-JL and DP-Adam-JL. The acceleration is achieved by only approximately instead of exactly computing the per-sample gradient norms. This does not affect the clipping operation afterwards and hence we can replace the local clipping currently used by our global clipping.

Algorithm 4 DP-SGD-JL (with local or global per-sample clipping)

Input: Dataset $S = \{(\mathbf{x}_1, y_1), \dots, (\mathbf{x}_n, y_n)\}$, loss function $\ell(f(\mathbf{x}_i, \mathbf{w}_t), y_i)$.

Parameters: initial weights \mathbf{w}_0 , learning rate η_t , subsampling probability p , number of iterations T , noise scale σ , gradient norm bound R , maximum norm bound Z , number of JL projections r .

```
for  $t = 0, \dots, T - 1$  do
  Take a subsample  $I_t \subseteq \{1, \dots, n\}$  from training set  $D$  with subsampling probability  $p$ 
  Sample  $u_1, \dots, u_r \sim \mathcal{N}(0, I)$ 
  for  $i \in I_t$  do
     $v_t^{(i)} \leftarrow \nabla_{\mathbf{w}} \ell(f(\mathbf{x}_i, \mathbf{w}_t), y_i)$ 
    for  $j = 1$  to  $r$  do
       $P_{ij} \leftarrow v_t^{(i)} \cdot u_j$  (using jvp)
     $M_i = \sqrt{\frac{1}{r} \sum_{j=1}^r P_{ij}^2}$  ▷  $M_i$  is an estimate for  $\|v_t^{(i)}\|_2$ .
    Option 1:  $C_{local,i} = \min \{1, R/M_i\}$  ▷ Local clipping factor
    Option 2:  $C_{global,i} \equiv \begin{cases} R/Z & \text{if } M_i \leq Z \\ 0 & \text{if } M_i > Z \end{cases}$ 
     $\bar{v}_t^{(i)} \leftarrow C_i \cdot v_t^{(i)}$  ▷ Clip the gradient
   $\bar{V} \leftarrow \sum_{i \in I_t} \bar{v}_t^{(i)}$  ▷ Sum over batch
   $\tilde{V}_t \leftarrow \bar{V}_t + \sigma R \cdot \mathcal{N}(0, I)$  ▷ Apply Gaussian mechanism
   $\mathbf{w}_{t+1} \leftarrow \mathbf{w}_t - \frac{\eta_t}{|I_t|} \tilde{V}_t$  ▷ Descend
```

Output \mathbf{w}_T

In another line of research on the Bayesian neural networks, where the reliability of networks are emphasized, stochastic gradient Markov chain Monte Carlo (SG-MCMC) methods are applied to quantify the uncertainty of the weights. When DP is within the scope, one popular method is the DP stochastic gradient Langevin dynamics (DP-SGLD), where we can apply the global clipping.

Algorithm 5 DP-SGLD (with local or global per-sample clipping)

Input: Dataset $S = \{(\mathbf{x}_1, y_1), \dots, (\mathbf{x}_n, y_n)\}$, loss function $\ell(f(\mathbf{x}_i, \mathbf{w}_t), y_i)$.

Parameters: initial weights \mathbf{w}_0 , learning rate η_t , subsampling probability p , number of iterations T , gradient norm bound R , maximum norm bound Z , and a prior $p(\mathbf{w})$.

```
for  $t = 0, \dots, T - 1$  do
  Take a subsample  $I_t \subseteq \{1, \dots, n\}$  from training set  $D$  with subsampling probability  $p$ 
  for  $i \in I_t$  do
     $v_t^{(i)} \leftarrow \nabla_{\mathbf{w}} \ell(f(\mathbf{x}_i, \mathbf{w}_t), y_i)$ 
    Option 1:  $C_{local,i} = \min \{1, R/\|v_t^{(i)}\|_2\}$  ▷ Local clipping factor
    Option 2:  $C_{global,i} \equiv \begin{cases} R/Z & \text{if } \|v_t^{(i)}\|_2 \leq Z \\ 0 & \text{if } \|v_t^{(i)}\|_2 > Z \end{cases}$  ▷ Global clipping factor
     $\bar{v}_t^{(i)} \leftarrow C_i \cdot v_t^{(i)}$  ▷ Clip the gradient
   $\bar{V} \leftarrow \sum_{i \in I_t} \bar{v}_t^{(i)}$  ▷ Sum over batch
   $\mathbf{w}_{t+1} \leftarrow \mathbf{w}_t - \eta_t \left( \frac{\bar{V}_t}{|I_t|} - \frac{\nabla_{\mathbf{w}} \log p(\mathbf{w})}{n} \right) + \mathcal{N}(0, \eta_t I)$  ▷ Descend with Gaussian noise
```

Output \mathbf{w}_T

Here we treat \mathbf{w}_{t+1} as a posterior sample, instead of as a point estimate. Notice that other SG-MCMC methods such as SGNHT [21] can also be DP with the global per-sample clipping.

We emphasize that our global clipping applies whenever an optimization algorithm uses per-sample clipping. Therefore this appendix only gives a few example of the full capacity of global clipping.

F.5 Applying Global Clipping to DP Federated Learning

Here we present two federated learning methods in [38]: DP-FedSGD and DP-FedAvg with the global or local clipping. Notice that we only demonstrate the flat clippings and SGD. Layerwise clippings can be easily implemented by changing the ClipFn, and the optimizer can be replaced by other ones.

<p>Main training loop:</p> <p><i>parameters</i></p> <ul style="list-style-type: none"> user selection probability $q \in (0, 1]$ number of examples per-user w_k gradient norm bound R maximum norm bound Z noise scale σ UserUpdate (for FedAvg or FedSGD) ClipFn (LocalClip or GlobalClip) <p>Initialize model θ^0, $W = \sum_k w_k$</p> <p>for each round $t = 0, 1, 2, \dots$ do</p> <ul style="list-style-type: none"> $\mathcal{C}^t \leftarrow$ (sample users with probability q) for each user $k \in \mathcal{C}^t$ in parallel do <li style="padding-left: 20px;">$\Delta_k^{t+1} \leftarrow$ UserUpdate(k, θ^t, ClipFn) <li style="padding-left: 20px;">$\Delta^{t+1} = \frac{\sum_{k \in \mathcal{C}^t} w_k \Delta_k}{qW}$ <li style="padding-left: 20px;">$\theta^{t+1} \leftarrow \theta^t + \Delta^{t+1} + \frac{\sigma}{qW} RN(0, I)$ 	<p>FlatClip(Δ):</p> <ul style="list-style-type: none"> return $\Delta \cdot \min\{1, R/\ \Delta\ _2\}$ <p>GlobalClip(Δ):</p> <ul style="list-style-type: none"> if $\Delta > Z$: <li style="padding-left: 20px;">return 0 else: <li style="padding-left: 20px;">return $\Delta \cdot R/Z$ <p>UserUpdateFedAvg(k, θ^0, ClipFn):</p> <ul style="list-style-type: none"> <i>parameters</i> B, E, η $\theta \leftarrow \theta^0$ for each local epoch i from 1 to E do <li style="padding-left: 20px;">$\mathcal{B} \leftarrow$ (k's data split into size B batches) <li style="padding-left: 20px;">for batch $b \in \mathcal{B}$ do <li style="padding-left: 40px;">$\theta \leftarrow \theta - \eta \nabla \ell(\theta; b)$ <li style="padding-left: 40px;">$\theta \leftarrow \theta^0 + \text{ClipFn}(\theta - \theta^0)$ return update $\Delta_k = \theta - \theta^0$ <p>UserUpdateFedSGD(k, θ^0, ClipFn):</p> <ul style="list-style-type: none"> <i>parameters</i> B, η select a batch b of size B from k's examples return update $\Delta_k = \text{ClipFn}(-\eta \nabla \ell(\theta; b))$
--	--

Algorithm 6: DP-FedAvg and DP-FedSGD with global or local clipping.

F.6 Comparison between Different Clippings

Here we give a brief comparison between different clippings: the local per-sample clipping, the global per-sample clipping and the non-DP batch clipping (see Algorithm 7). In the example of SGD, the key difference between

Algorithm 7 Non-DP SGD (with batch clipping)

for $t = 0, \dots, T - 1$ **do**

- Take a subsample $I_t \subseteq \{1, \dots, n\}$ from training set D with subsampling probability p
- for** $i \in I_t$ **do**
- $v_t^{(i)} \leftarrow \nabla_{\mathbf{w}} \ell(f(\mathbf{x}_i, \mathbf{w}_t), y_i)$
- $V_t \leftarrow \frac{1}{|I_t|} \sum_{i \in I_t} v_t^{(i)}$ \triangleright Sum over batch
- $\bar{V}_t \leftarrow V_t \cdot \min\{1, R'/\|V_t\|_2\}$ \triangleright Clip the gradient
- $\mathbf{w}_{t+1} \leftarrow \mathbf{w}_t - \eta_t \bar{V}_t$ \triangleright Descend

Output \mathbf{w}_T

the non-DP clipping and the DP clippings is the order of operations: the non-DP clipping first average the per-sample gradients, then clips in a batch manner. However, for DP clippings in Algorithm 1, we first clip the per-sample gradients (the local clipping works in a per-sample manner but the global clipping works in a batch manner) then take the average of the clipped gradients. Informally, we distinguish the gradients after different clippings as follows:

- **non-DP batch clipping:** $\bar{V}_t = \text{ave}(v_t^{(i)}) \cdot c' = \text{ave}(v_t^{(i)} \cdot c')$;
- **DP local per-sample clipping:** $\bar{V}_t = \text{ave}(v_t^{(i)} \cdot C_i)$;

- **DP global per-sample clipping:** $\bar{V}_t = \text{ave}(v_t^{(i)} \cdot C)$;

where $0 < c', C, C_i \leq 1$ are clipping factors and ‘ave’ is the average. Notice that $C = R/Z$ and hence even though the global clipping is performing a batch clipping, it still requires the $|I_t|$ per-sample clipping factors (which needs to compute the per-sample gradients and their norms) and hence is different from non-DP batch clipping. See Table 4.

	non-DP clipping	DP local clipping	DP global clipping
Need per-sample gradient	No	Yes	Yes
Batch clipping	Yes	No	Yes

Table 4: Comparison of different clippings with respect to whether per-sample gradient information is needed and whether the operation can be applied on the batch as a whole.